

# Extinctions of coupled populations, and rare-event dynamics under non-Gaussian noise

Tal Agranov and Guy Bunin

*Department of Physics, Technion—Israel Institute of Technology, Haifa 3200003, Israel*

The survival of natural populations may be greatly affected by environmental conditions that vary in space and time. We look at a population residing in two locations (patches) coupled by migration, in which the local conditions fluctuate in time. We report on two findings. First, we find that unlike rare events in many other systems, here the histories leading to a rare extinction event are not dominated by a single path. We develop the appropriate framework, which turns out to be a hybrid of the standard saddle-point method, and the Donsker-Varadhan formalism which treats rare events of atypical averages over a long time. It provides a detailed description of the statistics of histories leading to the rare event, and the mean time to extinction. The framework applies to rare events in a broad class of systems driven by non-Gaussian noise. Secondly, applying this framework to the population-dynamics model, we find a novel phase transition in its extinction behavior. Strikingly, a patch which is a sink (where individuals die more than are born), can nonetheless reduce the probability of extinction, even if it normally lowers the population's size and growth rate.

The extinction of populations extended over space is a central question in evolution, ecology and conservation that has been studied extensively both theoretically and empirically [1–19]. Environmental conditions, that vary in space and time, can play an important role in the survival of these populations [7–12, 14–19].

Here we look at a model of a population residing in two locations (patches), coupled by migration, and experiencing environmental fluctuations, modeled by noisy growth rates [20–22]. Whereas the extinction of a single isolated population is well understood [4–6, 13], much less is known about extinctions in the two-patch system. We present a comprehensive analytical treatment of this long-standing problem, that holds a number of surprises.

We find a counter-intuitive effect, at small migration rates, where the existence of *sink* patches (where more individuals die than are born) may reduce the probability of extinction, by effectively acting as sources during a potential extinction event. Thus patches can offer significant protection against extinction even if they have little or detrimental effect on the population size and growth rates, which are common ecological criteria for survival [23–26]. The edge of the regime where this happens is marked by a sharp, dynamical phase transition, along with non-analyticity in the large deviation function.

We develop a formalism to derive these and other results. The theory of rare events provides powerful tools to determine the likelihood of extinctions, and how and why they might occur [3–5]. In many systems, rare states such as extinction are reached by a single system history, with negligible probability for all other paths. The formalism used to find this path and its probability is known by various names such as the instanton method (IM), or dissipative WKB [27, 28].

Yet, we find that extinction events in the two-patch model, as well as rare events in an entire class of other problems that we identify, are *not* reached by a single path as in the IM. To treat this problem, we invoke a different class of rare events, that occur when the long-time

average of a given observable attains an atypical value [28]. Their dynamics are fundamentally different, where a collection of paths are likely, rather than a single one. They are described by the established Donsker-Varadhan (DV) formalism [28–35]. We find that extinction events can be viewed as a *combination* of the above two classes of rare events, and formulate a hybrid framework that accounts for it, combining the DV and IM formalisms. It allows to evaluate the probability of a rare event, and also to fully characterize the ensemble of system paths which lead to its realization.

The broader class of problems amenable to this formalism includes many systems experiencing colored and in particular non-Gaussian noise, e.g. [20–22, 36–47], sometimes appearing in conjunction with a noise-induced stabilization effect [14, 16, 20–22, 41, 48–50]. Within this class, works on specific models provided numerical or partial analytic results [16, 21, 37, 39, 49], while others [36, 38, 45–48] obtained the probability of rare events using the specialized form of certain models. We show how to treat the general case and fully characterize the fluctuating dynamics leading to the rare event.

*Extinction of coupled population patches.* Consider two patches harboring populations of sizes  $N_{1,2}(t)$ , which grow at rates  $r_{1,2}$  at low abundance, and reach a single fixed point at the carrying capacity  $K_{1,2}$ .  $K_{1,2}$  serve as the largest parameter in our problem, and we assume that they both scale with a single large parameter, say  $K \equiv (K_1 + K_2)/2 \gg 1$ . The two patches are then coupled by migration. Assuming the dynamics is also subject to white environmental noise, and for large populations where  $N_{1,2}(t)$  can be treated as continuous variables, it is described by the coupled Langevin equations [4, 5, 38]

$$\begin{aligned}\dot{N}_1 &= r_1 N_1 [1 - h_1(N_1)] + D(N_2 - N_1) + N_1 \sigma \eta_1, \\ \dot{N}_2 &= r_2 N_2 [1 - h_2(N_2)] + D(N_1 - N_2) + N_2 \sigma \eta_2.\end{aligned}\quad (1)$$

Here  $D$  is the coupling strength and  $h$  is a regulating term which ensures the growth rates vanish in an isolated patch when  $N_i = K_i$ , such as the logistic term  $h = N/K$ ,

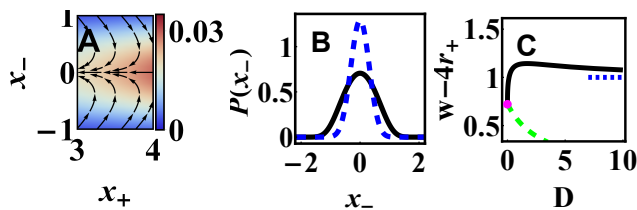


Figure 1. (A) The stationary joint probability distribution  $P_s(x_+, x_-)$  corresponding to the dynamics (3)-(4), with reflecting boundary conditions at  $x_+ = \ln K = 10$ ; The arrows show the deterministic force; Parameters are  $r_1 = r_2 = -0.2$  and  $D = 0.3$ . The arrows pointing left on the  $x_+$  axis, show that the noiseless dynamics would lead to extinction, yet the average growth rate is positive,  $r_+ + \langle g \rangle = 0.102$ . (B) The  $x_-$  distribution during typical growth (5) (solid line), is narrower during an extinction event (dashed line). Both obtained analytically, at  $r_+ = 2.402$ . (C) The exponent  $W$  as a function of the coupling strength  $D$  for  $r_1 = 2.2$  and  $r_2 = 0.2$ , together with the high and low asymptotic values in blue dotted line and magenta circle respectively. The green dashed line is the incorrect IM prediction.

but its exact form is irrelevant when addressing extinctions, as their likelihood is dominated by the dynamics away from the fixed point. The right-most terms in Eq. (1) model the effect of fluctuating conditions on growth rates [3, 4, 20], where  $\eta_i(t)$  are zero-mean Gaussian white noises  $\langle \eta_i(t) \eta_j(t') \rangle = \delta_{i,j} \delta(t - t')$ , for  $i, j = 1, 2$  [51].

This model and its various extensions has received much attention recently [20–22]. Much is known about its *typical* behavior—i.e. unconditioned on a rare event like extinction—but far less about extinctions. An equivalent problem appears in economics [41], evolution [50], and as a model of a diverse ecosystem, where a species' growth rate fluctuates due to the influence of others [52].

The dynamics (1) leads to a stationary distribution  $P_s$ , peaked around the carrying capacity  $N_i = K_i \gg 1$ , see Fig. 1(A). Yet the system can also reach a small number of individuals  $N_i \sim \mathcal{O}(1)$  via a rare noise realization. There the continuous description (1) breaks down, and demographic noise may bring the system to extinction,  $N_1 = N_2 = 0$ . To leading order, the mean time to extinction (MTE) is given by  $1/P_s(N_1 = N_2 = 1)$  [4, 38, 53].

We begin the discussion with uncoupled populations,  $D = 0$ , where the problem reduces to the classical single patch system [4]. Here the MTE has a power law dependence on the carrying capacity,  $\text{MTE} \sim K^{2r/\sigma^2}$  at large  $K$ , see e.g. [6, 13]. The exponent  $2r/\sigma^2$  will be our focus in the following, as it significantly affects the MTE when  $K$  is large. One simple way of arriving at this result is by going over to the logarithmic coordinate  $x = \ln N$ , which performs simple biased diffusion  $\dot{x} \simeq r + \sigma \eta$  when not too close to the metastable fixed point. The abundance at extinction, where there are  $N \sim \mathcal{O}(1)$  individuals, corresponds to  $x = 0$ . Then the MTE is given by the Arrhenius formula for the mean time for  $x$  to cross an energy barrier of height  $r \ln K \gg \sigma^2$  between the metastable fixed point  $x = \ln K$  and the stable extinction  $x = 0$ .

The barrier crossing probability is given by that of the most probable path, using the standard IM [27, 28, 38]. As the Langevin dynamics of a single patch obeys detailed balance, the optimal path is given by the time-reversal of the typical dynamics, i.e., following a simple decline at the constant rate  $r_d = r$  over the long decline time  $T = \ln K/r$  [38]. Thus for a single patch, the typical growth, the decline rate  $r_d$ , and the extinction probability are all controlled by the single parameter  $r$ . As we now show, when coupling two such population patches, the simple IM treatment fails, a different extinction mechanism comes into play and these three rates are different from one another.

Starting from the coupled dynamics (1), it is helpful to switch to logarithmic coordinates  $x_i = \ln N_i$ . We also rescale  $D \rightarrow D/\sigma^2$ ,  $r_i \rightarrow r_i/\sigma^2$  and  $t \rightarrow t\sigma^2$ , resulting in unit noise amplitude  $\sigma^2 = 1$ ; the  $\sigma$  dependence can always be restored from dimensional considerations. For  $x_{1,2}$  smaller than, and not very close to  $\ln K$ , the regulating term  $h$  is negligible and one obtains

$$\begin{aligned} \dot{x}_1 &= r_1 + D(e^{x_2 - x_1} - 1) + \eta_1, \\ \dot{x}_2 &= r_2 + D(e^{x_1 - x_2} - 1) + \eta_2. \end{aligned} \quad (2)$$

Now introduce the sum and difference coordinates  $x_{\pm} = (x_1 \pm x_2)/2$ , for which

$$\dot{x}_+ = r_+ + 2D \sinh^2 x_- + \eta_+/\sqrt{2}, \quad (3)$$

$$\dot{x}_- = r_- - D \sinh 2x_- + \eta_-/\sqrt{2}. \quad (4)$$

Here  $r_{\pm} \equiv (r_1 \pm r_2)/2$ , and  $\eta_-$  and  $\eta_+$  are zero mean and unit variance uncorrelated Gaussian white noises. We assume without loss of generality that  $r_- \geq 0$ . Extinction of the population in both patches corresponds to  $x_+ = 0$ .

Note that  $x_+(t)$  follows single-patch dynamics, with growth rate  $r_+$ , a Gaussian noise of magnitude  $1/\sqrt{2}$ , and an additional fluctuating supplement growth rate  $0 \leq g(t) \equiv 2D \sinh^2 x_-$  that originates from migration between the patches. This non-Gaussian colored noise term can be identified as the source of the failure of the IM, thus requiring a new approach. This is clearly seen in the fact that the system can sustain a stable population even when both patches have negative growth rates  $r_1 = r_2 \leq 0$ , provided that  $r_+ + \langle g \rangle \geq 0$ . Here the average is taken with respect to the steady state  $x_-$  distribution, which is reached during the long growth of  $x_+$  towards the carrying capacity

$$P_-(x_-) = \mathcal{N} e^{-4(D \cosh^2 x_- - r_- x_-)}, \quad (5)$$

where  $\mathcal{N}$  is a normalization constant (see Fig. 1(B)). This is the celebrated noise-induced stabilizing effect, where fluctuations and migration conspire to stabilize the coupled populations [14, 17, 20, 22]. As the IM ignores fluctuations around the optimal path, this crucial effect is completely missed by the IM treatment which erroneously predicts that the typical dynamics would decline rapidly to extinction if  $r_+ < 0$ . The mechanism behind this effect is clearly seen in a phase-space portrait of the dynamics (3)-(4) presented in Fig. 1(A).

Thus, fluctuations in  $x_-$  contribute to the positive supplement growth rate  $g$ , adding to the value of  $r_+$  and helping to stabilize  $x_+$ . One therefore expects that during extinction fluctuations in  $x_-$  will be suppressed in order to facilitate the decline of  $x_+$ , see Fig. 1(B). This effect is beyond the IM treatment, and accounted for by combining the IM and DV formalisms, as is now shown.

In the first step of the derivation we find the probability for extinction at time  $T$ , namely to reach  $x_+ = 0$  starting from the carrying capacity  $x_+(t=0) = \ln K$ , conditioned on a given  $x_-(t)$  trajectory. With this conditioning, Eq. (3) describes Brownian motion under the fixed time-dependent drift  $r_+ + g(t)$ . Extinction at time  $T$  corresponds to a generalized Brownian bridge between  $x_+(t=0) = \ln K$  and  $x_-(t=T) = 0$  [54]. As in the single-patch problem, this process is dominated in the large  $K$  limit by the optimal IM trajectory, which gives the conditional extinction probability at time  $T$  [54]

$$-\ln P[x_+(T) = 0|x_-] \simeq \ln K (r_d + G + r_+)^2 / r_d. \quad (6)$$

Here  $r_d = \ln K/T$  is the decline rate, and

$$G \equiv \frac{2D}{T} \int_0^T \sinh^2 x_- dt' \quad (7)$$

is the time average of the supplement growth rate  $g$  along the extinction path. Note that the probability cost (6) only depends on the  $x_-$  history via the time average (7).

We are left with the task of evaluating the probability cost  $P(G, T)$  of trajectories  $\{x_-(t)\}$  with a given time average value  $G$  (7). Importantly, as our IM scaling suggests (and is also verified self-consistently in the following) the decline time  $T$  scales as  $\ln K$ , and is thus very long. Fluctuations of long-time averaged (or empirical) observables is a classic subject in large deviation theory [28, 35]. Following a large deviation principle, this probability cost decays exponentially with time

$$-\ln P(G, T) \simeq T f(G). \quad (8)$$

$f$  is a convex rate function that attains its minimum at the average value  $G = \langle G \rangle$ , which also coincides with the average of the instantaneous supplement growth rate with respect to the stationary distribution (5),  $\langle G \rangle = \langle g \rangle$ .

Combining the results, as both the conditional probability (6), and the DV cost (8) scale exponentially with  $\ln K$ , then by the contraction principle [28], the extinction probability is given to leading order by  $-\ln P(x_+ = 0) \simeq W \ln K$ .  $W$  is the minimum over  $G$  and decline rate  $r_d$  of the combined probability cost

$$W = \min_{G, r_d} \left[ (r_d + G + r_+)^2 + f(G) \right] / r_d. \quad (9)$$

Finally, the MTE grows as a power law of the carrying capacity  $\text{MTE} \sim K^W$ . Fig. 1(C) shows  $W$  as a function of the coupling strength  $D$ .

The rate function  $f$  is obtained by the established DV formalism [28–35] reviewed with application to our problem in the Supplemental Material [54]. In short, this

problem reduces to finding the ground state of a one-dimensional Schrödinger equation. Importantly, in addition to the rate function  $f$ , the DV formalism gives the dynamics of the process conditioned on the time average (7), apart from short times at the start and end of the process, as a Langevin process with a known modified potential  $V_G$  that biases the dynamics to realize the constraint (7)

$$\dot{x}_-^c = -V_G'(x_-^c) + \eta_- / \sqrt{2}. \quad (10)$$

The dynamics of  $x_+$  conditioned on extinction,  $x_+^c$ , follows from mapping to a Brownian bridge [54]

$$\dot{x}_+^c = -\frac{x_+^c}{T-t} + \frac{\eta_+}{\sqrt{2}} + \eta_g, \quad (11)$$

where  $T = \ln K/r_d$ , and  $\eta_g = 2D \sinh^2 x_-^c - G$  is a zero-mean non-Gaussian noise term that captures the fluctuations in the supplement growth rate  $g$  during extinction.

Eqs. (10)-(11) provide a complete statistical characterization of the trajectories conditioned on extinction. It predicts that extinction is reached by one of a *collection of extinction trajectories*, in which the coordinates  $x_{1,2}$  decline together at a rate  $r_d$ , while their difference fluctuates according to the stationary process (10). This is in contrast to the usual IM treatment where only the most probable extinction trajectory is relevant.

Using this framework, we now discuss the regimes of small and large migration coupling. At strong coupling  $D \rightarrow \infty$ , the extinction of the coupled populations is equivalent to that of a single patch, as one might expect, with growth rate  $r_+ + \langle G \rangle$  and half the noise variance, so that  $W = 4(r_+ + \langle G \rangle) + \mathcal{O}(D^{-1})$ , with  $\langle G \rangle \rightarrow 1/4$  [54].

The opposite limit of small coupling,  $D \rightarrow 0^+$ , reveals rich and unexpected behavior. Consider first the typical behavior. Typical growth of the total population by Eq. (2) is dominated by the larger growth  $r_1$ , ( $r_1 > r_2$ ). Patch 2 contains only a small fraction of the population, and so has negligible effect on the mean and variance of the growth rate, or the final total population size. Noise-induced stabilization is negligible [20, 54]. Patch 2 might therefore seem to have little bearing on the chances of extinction, as suggested by common ecological criteria [23–26], and perhaps even a detrimental effect if it is a sink ( $r_2 < 0$ ).

Yet we find that even sink patches can significantly reduce the chances of extinction, via a finite ( $\mathcal{O}(D^0)$ ) effect on  $W$ . This happens in one of two regimes in  $r_1, r_2$ , with two qualitatively distinct dynamics preceding extinction.

The *extinction sink* regime occurs when  $r_2 < -r_1$ . It is instructive to first look at uncoupled ( $D = 0$ ) patches. During extinction, patch 1 declines at rate  $-r_1$ , and patch 2 declines even without conditioning, and at a faster rate than  $-r_1$ . The effect of small  $D > 0$  on extinction is to slow the decline of patch 2 to match that of patch 1, with a much smaller population in patch 2 than in patch 1,  $x_-^c \sim \ln(|r_+|/D)$  (Fig. 2(A,C)). This allows migration into patch 2, normalized by population size, to

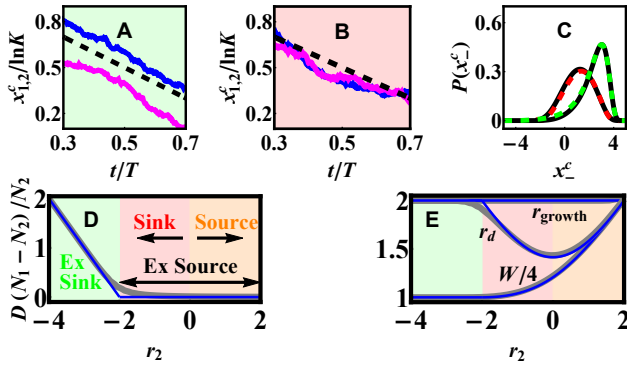


Figure 2. Extinction at small coupling  $D$ . (A,B) A realization of extinction trajectories for  $x_1^c$  in blue and  $x_2^c$  in magenta generated from the process (10)-(11). At (A) the extinction sink regime and (B) extinction source regime, for a sink patch 2,  $r_2 < 0$ . Dashed lines show the predicted decline rate. (C) The corresponding stationary distribution of  $x_-^c$ , the  $x_-$  coordinate conditioned on extinction (solid lines), together with the analytical prediction in the extinction sink (red) and extinction source regimes (green). (D) Migration into patch 2 during extinction, normalized by population size, for  $r_1=2$ . (E) The extinction probability exponent  $W$ , decline rate  $r_d$  and growth rate, for  $r_1=2$ . Note that in the extinction sink regime  $r_2 < -r_1$ ,  $W=4$  as for patch 1 alone, and migration into patch 2 is non-negligible; while in the extinction source regime  $-r_1 < r_2$  the extinction probability is suppressed  $W > 4$  and the migration vanishes, both when patch 2 is a sink,  $r_2 < 0$ , or a source. In (D,E) the thin blue lines are analytical predictions for  $D \rightarrow 0^+$ , and the thicker gray lines for  $D = 10^{-3}$ ; in (A)  $r_1 = 4, r_2 = -4.41, D = 10^{-3}$ ; in (B)  $r_1 = 4, r_2 = -3.47, D = 10^{-3}, \ln K = 20$ .

reach a finite value  $\langle D(N_1 - N_2)/N_2 \rangle_c \simeq |r_+|$ , see Fig. 2(D) (here  $\langle \dots \rangle_c$  denotes an average with respect to the conditioned dynamics (10)). Meanwhile, the extinction in patch 1 proceeds with little effect of migration from the small population in patch 2. This picture is made precise by showing that the dynamics towards extinction (10)-(11) become

$$\dot{x}_1^c = -\frac{x_1^c}{T-t} + \eta_1, \quad (12)$$

$$\dot{x}_2^c = r_2 + D \left( e^{x_1^c - x_2^c} - 1 \right) + \eta_2, \quad (13)$$

with  $T = \ln K/r_1$  [54]. That is,  $x_1^c$  heads to extinction at rate  $r_d = r_1$  as if migration is absent (a Brownian bridge), while the  $x_2^c$  dynamics are unconditioned, except for the migration from patch 1, with given  $x_1^c$  trajectories.

In the *extinction source* regime,  $-r_1 < r_2 < r_1$ , the extinction of an uncoupled patch 1 would proceed at the rate  $-r_1$ , which is more negative than the typical growth rate in patch 2 alone,  $\langle \dot{x}_2 \rangle = r_2 \geq -r_1$ . Thus, when coupled, extinction now also requires unfavorable conditions in patch 2, *lowering* the chance of extinction. Strikingly, this includes a regime where  $r_2$  is negative  $-r_1 < r_2 < 0$ , and during normal growth acts as a *sink*. The difference distribution for  $x_-^c$  in this regime is spread around the origin over a large scale  $\sim |\ln D|$ ,

see Figs. 2(B,C). Although this distribution is wide, its average is finite and the migration to patch 2 vanishes to leading order,  $\langle D(N_1 - N_2)/N_2 \rangle_c = \mathcal{O}(1/|\ln D|)$  (Fig. 2(D)). In this sense patch 2 is *no longer a sink* during extinction. The decline rate also depends on both  $r_1, r_2$ ,  $r_d = \sqrt{(r_1^2 + r_2^2)}/2$ .

The transition between these two regimes leads to a phase transition (discontinuous second derivative) in the extinction probability exponent, see Fig. 2(E),

$$W = \begin{cases} r_1 + r_2 + \sqrt{2(r_1^2 + r_2^2)}, & |r_2| \leq r_1, \\ 2r_1, & r_2 \leq -r_1. \end{cases} \quad (14)$$

In the extinction source regime, patch 2 acts against extinction much like a source, while extinction sink result (15) comes solely from contribution of patch 1.

An IM evaluation of  $W$  turns out to reproduce the correct result (14)-(15) at small  $D$ , see Fig. 1(C): in the extinction sink regime (15) only patch 1 contributes, acting like a single-patch decline. In the extinction source regime (14) migration is negligible, and extinction corresponds to the simultaneous decline of two single patches, correctly captured by IM, under the additional constraint that the two patches decline together to zero.

*Broader applicability.* Colored, and in particular non-Gaussian noise is often generated by an autonomous process, see e.g. [20–22, 36–49]. A prototypical model of this family features a “reaction coordinate”  $x_+$  driven both by Gaussian noise and an additional non-Gaussian colored noise  $x_-$

$$\begin{aligned} \dot{x}_+ &= -U'(x_+) + g(x_-) + \sigma_+ \eta_+, \\ \dot{x}_- &= -V'(x_-) + \sigma_- \eta_-. \end{aligned} \quad (16)$$

Previous works that examined rare events within the family (16) [16, 21, 36–38, 42, 45–48], give partial or no analytical analysis, or calculate  $W$  for specialized forms of (16), such as linear  $V'$  or  $g$  [36, 38, 45–48], without addressing the generic case or providing the fluctuating dynamics conditioned on extinction as in Eqs.(10)-(11).

We look at rare events of (16) in which the reaction coordinate  $x_+$  reaches a large potential difference  $\Delta U/\sigma_+^2 \gg 1$ . First, for constant  $U'(x_+)$ , the derivation above can be readily followed, merely by substituting  $2D \sinh^2 x_- \rightarrow g$  and  $D \sinh 2x_- - r_- \rightarrow V'$ . As above, *given an  $x_-$  trajectory*, one can evaluate the probability of  $x_+$  histories using the IM formalism. However, the accompanying  $x_-$  trajectories are not dominated by a single path and IM is inapplicable, as in general the rare event is not characterized by large potential difference for the  $x_-$  coordinate,  $\Delta V/\sigma_-^2 \not\gg 1$ . However, if the time scale of the rare  $x_+$  history is much larger than the relaxation time of  $x_-$  in the potential  $V$ , then the accompanying  $x_-$  histories can be fully characterized by the DV formalism. The extension to non-constant  $U'(x_+)$  proceeds by dividing the  $x_+$  trajectory to small pieces, where  $U'$  can be taken as constant [48, 54].

*Acknowledgments*—G. Bunin acknowledges support by the Israel Science Foundation (ISF) Grant no. 773/18.

- 
- [1] M. S. Bartlett, *Stochastic Population Models; in Ecology and Epidemiology*, Tech. Rep. (1960).
- [2] R. M. Nisbet and W. Gurney, *Modelling Fluctuating Populations: Reprint of First Edition (1982)* (2003).
- [3] R. Lande, S. Engen, and B.-E. Saether, *Stochastic Population Dynamics in Ecology and Conservation* (Oxford University Press, 2003).
- [4] O. Ovaskainen and B. Meerson, *Trends in Ecology & Evolution* **25**, 643 (2010).
- [5] M. Assaf and B. Meerson, *Journal of Physics A: Mathematical and Theoretical* **50**, 263001 (2017).
- [6] E. G. Leigh Jr, *Journal of Theoretical Biology* **90**, 213 (1981).
- [7] J. A. J. Metz, T. J. De Jong, and P. G. L. Klinkhamer, *Oecologia* **57**, 166 (1983).
- [8] R. D. Holt, *Theoretical population biology* **28**, 181 (1985).
- [9] D. P. Hardin, P. Takáč, and G. F. Webb, *Journal of Mathematical Biology* **26**, 361 (1988).
- [10] D. P. Hardin, P. Takáč, and G. F. Webb, *SIAM Journal on Applied Mathematics* **48**, 1396 (1988).
- [11] S. Harrison and J. F. Quinn, *Oikos* , 293 (1989).
- [12] D. P. Hardin, P. Takáč, and G. F. Webb, *Journal of mathematical biology* **28**, 1 (1990).
- [13] R. Lande, *The American Naturalist* **142**, 911 (1993).
- [14] V. A. A. Jansen and J. Yoshimura, *Proceedings of the National Academy of Sciences* **95**, 3696 (1998).
- [15] M. Roy, R. D. Holt, and M. Barfield, *The American Naturalist* **166**, 246 (2005).
- [16] R. Abta, M. Schiffer, and N. M. Shnerb, *Physical review letters* **98**, 098104 (2007).
- [17] D. P. Matthews and A. Gonzalez, *Ecology* **88**, 2848 (2007).
- [18] S. J. Schreiber, *Proceedings of the Royal Society B: Biological Sciences* **277**, 1907 (2010).
- [19] B. Ottino-Löffler and M. Kardar, arXiv preprint arXiv:2007.11749 (2020), arXiv:2007.11749.
- [20] S. N. Evans, P. L. Ralph, S. J. Schreiber, and A. Sen, *Journal of Mathematical Biology* **66**, 423 (2013).
- [21] H. Hakoyama and Y. Iwasa, *Journal of Theoretical Biology* **232**, 203 (2005).
- [22] A. Hening, D. H. Nguyen, and G. Yin, *Journal of mathematical biology* **76**, 697 (2018).
- [23] R. W. Howe, G. J. Davis, and V. Mosca, *Biological Conservation* **57**, 239 (1991).
- [24] P. Chesson, *Theoretical population biology* **45**, 227 (1994).
- [25] P. Chesson, *Annual review of Ecology and Systematics* **31**, 343 (2000).
- [26] J. Pande, T. Fung, R. Chisholm, and N. M. Shnerb, *Ecology letters* **23**, 274 (2020).
- [27] M. I. Freidlin and A. D. Wentzell, in *Random Perturbations of Dynamical Systems* (Springer, 1998) pp. 15–43.
- [28] H. Touchette, *Physics Reports* **478**, 1 (2009).
- [29] M. D. Donsker and S. R. S. Varadhan, *Communications on Pure and Applied Mathematics* **28**, 279 (1975).
- [30] M. D. Donsker and S. R. S. Varadhan, *Communications on Pure and Applied Mathematics* **29**, 389 (1976).
- [31] M. D. Donsker and S. R. S. Varadhan, *Communications on Pure and Applied Mathematics* **36**, 183 (1983).
- [32] M. D. Donsker and S. R. S. Varadhan, *Communications on Pure and Applied Mathematics* **28**, 1 (2010).
- [33] J. Gärtner, *Theory of Probability & Its Applications* **22**, 24 (1977).
- [34] R. S. Ellis, *The Annals of Probability* **12**, 1 (1984).
- [35] H. Touchette, *Physica A: Statistical Mechanics and its Applications* **504**, 5 (2018).
- [36] M. M. Klosek-Dygas, B. J. Matkowsky, and Z. Schuss, *Journal of Statistical Physics* **54**, 1309 (1989).
- [37] S. Kitada, *Physica A: Statistical Mechanics and its Applications* **370**, 539 (2006).
- [38] A. Kamenev, B. Meerson, and B. Shklovskii, *Physical Review Letters* **101**, 268103 (2008).
- [39] A. Hutt, *EPL (Europhysics Letters)* **84**, 34003 (2008).
- [40] E. Barkai, E. Aghion, and D. A. Kessler, *Physical Review X* **4**, 021036 (2014).
- [41] J.-P. Bouchaud, *Journal of Statistical Mechanics: Theory and Experiment* **2015**, P11011 (2015).
- [42] U. Basu, S. N. Majumdar, A. Rosso, and G. Schehr, *Physical Review E* **100**, 062116 (2019).
- [43] E. Woillez, Y. Zhao, Y. Kafri, V. Lecomte, and J. Tailleur, *Physical Review Letters* **122**, 258001 (2019).
- [44] B. Walter, G. Pruessner, and G. Salbreux, arXiv:2006.00116 [cond-mat] (2020), arXiv:2006.00116 [cond-mat].
- [45] Y. Yahalom and N. M. Shnerb, *Physical Review Letters* **122**, 108102 (2019).
- [46] E. Woillez, Y. Kafri, and V. Lecomte, *Journal of Statistical Mechanics: Theory and Experiment* **2020**, 063204 (2020).
- [47] E. Woillez, Y. Kafri, and N. S. Gov, *Physical Review Letters* **124**, 118002 (2020).
- [48] M. Parker, A. Kamenev, and B. Meerson, *Physical Review Letters* **107**, 180603 (2011).
- [49] D. Valenti, A. Giuffrida, G. Denaro, N. Pizzolato, L. Curcio, S. Mazzola, G. Basilone, A. Bonanno, and B. Spagnolo, *Mathematical Modelling of Natural Phenomena* **11**, 158 (2016).
- [50] O. Peters and A. Adamou, arXiv preprint arXiv:1506.03414 (2015), arXiv:1506.03414.
- [51] We assume here without lose of generality the Stratonovich convention. In the Ito convention, the values of  $r_{1,2}$  in Eq. (3) and on, which enter in all the results below will be different from those in Eq. (1).
- [52] F. Roy, M. Barbier, G. Biroli, and G. Bunin, *PLoS computational biology* **16**, e1007827 (2020).
- [53] C. A. Braumann, *Computers & Mathematics with Applications* **56**, 631 (2008).
- [54] See Supplemental Material.
- [55] R. Chetrite and H. Touchette, *Physical review letters* **111**, 120601 (2013).
- [56] L. C. G. Rogers and D. Williams, *Diffusions, Markov Processes and Martingales, Volume 1: Foundations* (Chichester: Wiley, 1994).
- [57] M. H. Holmes, *Introduction to Perturbation Methods*, Vol. 20 (Springer Science & Business Media, 2012).
-

**SUPPLEMENTAL MATERIAL TO THE PAPER “EXTINCTIONS OF COUPLED POPULATIONS, AND RARE-EVENT DYNAMICS UNDER NON-GAUSSIAN NOISE” BY T. AGRANOV AND G. BUNIN**

**Table of contents**

- A. IM derivation of Eq. (6) for the  $x_+$  extinction.
- B. DV derivation of the rate function  $f$  and the conditioned process  $x_-^c$ .
- C. Derivation of the Eq. (11) using a mapping to a Brownian bridge.
- D. Solution of the DV problem in the strong coupling limit  $D \rightarrow \infty$ .
- E. Typical dynamics are dominated by the growth of uncoupled patch 1 in the weak migration limit  $D \rightarrow 0^+$ .
- F. Solution of the DV problem in the weak coupling limit  $D \rightarrow 0^+$ .
- G. Derivation of the conditioned dynamics, Eq. (12) and (13) in the weak coupling limit  $D \rightarrow 0^+$ .
- H. Rare events of the dynamics (16) for non constant  $U'$ .
- I. Two simplified forms of the dynamics (16) which can be treated by other methods.

**A. IM for the extinction of  $x_+$**

In this section we review the derivation of Eq. (6) of the main text using the IM.

Given a  $x_-$  trajectory, the  $x_+$  dynamics (3) is a simple biased diffusion, with a time-dependent drift, whose probability distribution can be found exactly, see Sec. C. However, being interested in the large  $K$  limit, we will employ here the IM which can only evaluate the extinction probability up to an exponential pre-factor. The advantage of the IM here, besides its simplicity, is that it can be straightforwardly extended to more involved cases with an  $x_+$  dependent forcing.

We start with the *conditional* probability path measure  $P[\{x_+(t)\} | \{x_-(t)\}]$  for observing the path history  $x_+(t)$  given a  $x_-(t)$  history. It is given, up to pre-exponential factors  $P[\{x_+(t)\} | \{x_-(t)\}] \propto e^{-S}$ , by the conditional path action

$$S[\{x_+(t)\} | \{x_-(t)\}] = \int_0^T (\dot{x}_+ - r - 2D \sinh^2 x_-)^2 dt'. \quad (\text{A1})$$

During an extinction,  $x_+$  declines from the large value  $\ln K$  to 0 during time  $T$ . To prove applicability of the IM we employ the re-scaling  $y_+ = x_+ / \ln K$  and  $\tau = t / \ln K$  and successfully isolate the large parameter  $\ln K$  in front of the conditional path measure  $S[\{y_+(\tau)\} | \{x_-(t)\}] = \ln K \int_0^{T/\ln K} (\partial_\tau y_+ - r_+ - 2D \sinh^2 x_-)^2 d\tau$ . Importantly, as the optimal extinction duration  $T$  scales also with  $\ln K$  as for the single patch case, then the  $\ln K$  dependence is pulled off from the integration limit. The large parameter  $\ln K$  in front of the conditional path measure makes the IM treatment for the conditional extinction valid here where the extinction event is dominated by the minimum action  $-\ln P[\{x_+(T) = 0\} | \{x_-(t)\}] \simeq S^*$ , evaluated over the optimal extinction path  $x_+$  (with  $x_+(0) = \ln K$  and  $x_+(t=T) = 0$ ) which minimizes the action (A1), see [27, 28]. Standard minimization yields Eq. (6)-(7) of the main text.

**B. The DV formalism for  $x_-$  during extinction**

Here we briefly review the DV formalism, as applied to the derivation of the rate function  $f$  from Eq. (8) and the conditioned dynamics, Eq. (10).

The DV formalism [29–32] reduces the problem of finding the rate function  $f(G)$ , defined in Eq. (8), to an effective eigenvalue problem. The rate function is given by a Legendre-Fenchel transform [33, 34]

$$f(G) = \max_k [kG - \xi(k)] \quad (\text{B1})$$

of the scaled cumulant generating function

$$\xi(k) = \lim_{T \rightarrow \infty} \frac{1}{T} \ln \langle e^{TkG} \rangle, \quad (\text{B2})$$

where  $\langle \dots \rangle$  denotes averaging over the process (4) of the main text. According to the DV method,  $\xi$  is the maximal eigenvalue of the operator  $\hat{L}^{(k)} \equiv \hat{L} + kg(x_-)$ , which is a tilted version of the Fokker-Planck generator  $\hat{L}$  corresponding to the Langevin equation for the stochastic process (4). The resulting eigenvalue problem reads

$$\frac{1}{4}h'' + [(D \sinh 2x - r_-)h] + 2kD \sinh^2 x h = \xi h, \quad (\text{B3})$$

with the boundary conditions  $h(x \rightarrow \pm\infty) = 0$ . Here and in the following the prime denotes the derivative with respect to the single argument. A usual protocol here is to make the operator in Eq. (B3) self adjoint by defining the operator  $\mathcal{H} = e^{-U/2} \hat{L}^{(k)} e^{U/2}$  where in our case  $U(x) = -\int^x 4(D \sinh 2x - r_-) = -4(D \cosh^2 x - r_- x)$ . This brings us to an effective Schrödinger equation

$$-\frac{1}{4}\psi'' + V_k \psi = -\xi \psi, \quad (\text{B4})$$

with the confining potential

$$V_k = (D \sinh 2x - r_-)^2 - D \cosh 2x - 2kD \sinh^2 x, \quad (\text{B5})$$

and where  $\xi(k)$  is minus the ground state energy. The two eigenfunctions are related via

$$\psi(x) = e^{2(D \cosh^2 x - r_- x)} h(x). \quad (\text{B6})$$

The solution of the eigenvalue problem also provides the process  $x_-^c$  conditional on the prescribed value of  $G$ , see e.e [55]. This process is also Markovian and is given by the Langevin Eq. (10) of the main text, with the biasing potential given by

$$V_G(x_-^c) = -\frac{1}{2} \ln \psi_k(x_-^c), \quad (\text{B7})$$

where  $k = k(G)$  is the argmax of the Legendre-Fenchel transform (B1) given by  $k(G) = f'(G)$ . The corresponding steady state distribution for  $x_-^c$ , conditioned on a prescribed value  $G$  than reads

$$P(x_-^c) = \mathcal{N} \psi_k^2(x_-^c), \quad (\text{B8})$$

where  $\mathcal{N}$  is a normalization constant. An example of the confining potential  $V_k$  (B5), and its associated ground state  $\psi_k$  is presented in Fig.3.

We note two points regarding the exponent  $W$  defined in Eq. (9). First, it can be found in terms of the cumulant generating function  $\xi$  and its argument  $k$ . Indeed, using the relation  $k(G) = f'(G)$ , and (B1) one can show that

$$W = -k. \quad (\text{B9})$$

with  $k$  the solution to the algebraic equation

$$\xi(k) + \frac{k^2}{4} + r_+ k = 0. \quad (\text{B10})$$

Second, it obeys the bounds

$$0 \leq W - 4r_+ \leq 4\langle G \rangle \quad (\text{B11})$$

The upper bound is given by the choice  $G = \langle G \rangle$  in Eq. (9) of the main text. For this value  $f = 0$  and we have the usual OFM extinction dynamics with the modified growth rate  $r_+ \rightarrow r_+ + \langle G \rangle$ . The lower bound is achieved by neglecting the cost of  $f$  altogether.

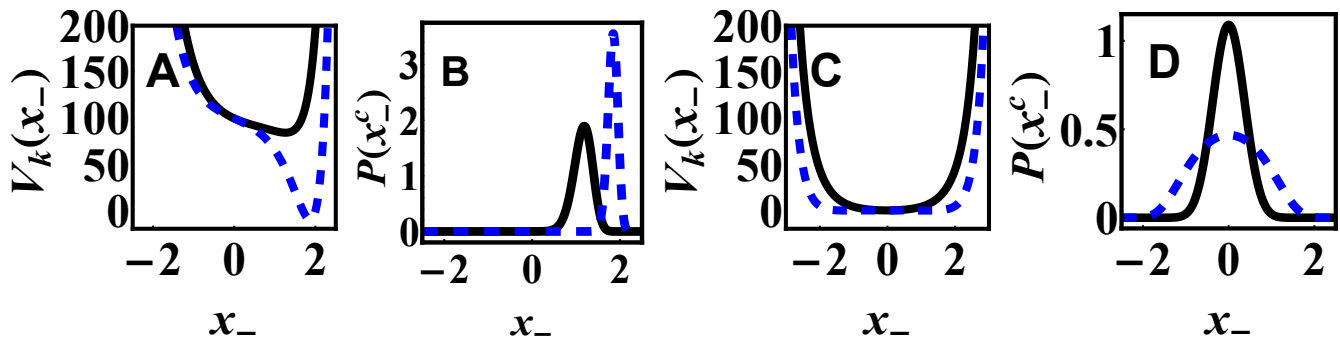


Figure 3. The confining potential  $V_k$  (B5) (A),(C) and its associated ground state  $\psi_k$  (B),(D) in thick black lines for  $k = -15$ . The dashed blue line correspond to  $k = 0$ , that is, the unconditional dynamics. In the left panels (A) and (B)  $r_- = 10$ , where the unconditional distribution is peaked away from the origin. For  $k < 0$ , the ground state eigenfunction's peak is advanced toward the origin, thus suppressing the value of  $G$  (7). In the right panels (C) and (D)  $r_- = 0$ , where the unconditional distribution is symmetric around the origin. The effect of  $k < 0$  here is to decrease the width of the eigenfunction which again suppresses the value of  $G$ . In all panels  $D = 0.1$ .

### C. The conditioned $x_+^c$ dynamics

Here we derive the conditioned  $x_+^c$  dynamics, Eq. (11).

Starting with Eq. (3) for  $x_+$ , define the stochastic variable  $y_+ = x_+ + r_+(T-t) + 2D \int_t^T \sinh^2 x_-(t') dt'$ , which follows pure Brownian motion

$$\dot{y}_+ = \frac{1}{\sqrt{2}}\eta_+. \quad (\text{C1})$$

The extinction of  $x_+^c$  during time  $T$  corresponds to a simple Brownian bridge  $y_+(t=0) = \ln K + (r_+ + G)T$ ,  $y_+(t=T) = 0$ , whose conditioned dynamics can be found, e.g., in [56]. Going back to  $x_+^c$ , we find:

$$\dot{x}_+^c = 2D \sinh^2 x_-(t) - \frac{\int_t^T 2D \sinh^2 x_-(t') dt'}{T-t} - \frac{x_+}{T-t} + \frac{\sigma}{\sqrt{2}}\eta_+. \quad (\text{C2})$$

As the accompanying  $x_-^c$  trajectories satisfy that the time average of  $g$  is equal to  $G$  for any macroscopic time interval, than Eq. (C2) give way to Eq. (11).

### D. Extinction in the strong coupling limit $D \rightarrow \infty$

Here we present the asymptotic solution of the DV problem (B4) at large  $D$ .

At large coupling we have that the two patches are infinitely coordinated, and fluctuations in  $G$  are significantly suppressed. Consequently we have that the rate function  $f$  diverges away from its minimum,  $f \simeq \tilde{f}(G)/\epsilon + \mathcal{O}(1)$  where  $\epsilon = 1/D$  is our small parameter. Correspondingly we have the scaling of the cumulant generating function (B2)  $\xi(k) = \tilde{\xi}(\tilde{k})/\epsilon$  with  $\tilde{k} = \epsilon k$ . The confining potential of the Schrödinger Eq. (B4) becomes vary narrow around its minimum  $x_{\min} = \mathcal{O}(\epsilon)$  which can be set to zero as it only contributes in the sub-leading order and the eigenfunction  $\psi$  is narrowly localized around the origin over a small scale  $x \sim 1/\sqrt{\epsilon}$ . Substituting  $\tilde{x} = \sqrt{\epsilon}x$ , and expanding in powers of  $\epsilon$  we have that Eq. (B4) becomes a simple quantum harmonic oscillator

$$\frac{1}{4}\partial_{\tilde{x}}^2\psi + \left[1 + (2\tilde{k} - 4)\tilde{x}^2 + \mathcal{O}(\epsilon)\right]\psi = \tilde{\xi}\psi. \quad (\text{D1})$$

The ground state is a Gaussian whose width is parameterized by  $\tilde{k}$ , which together with the ground state energy reads:

$$\psi(x) \simeq 2\sqrt{\frac{D\alpha}{\pi}}e^{-2D\alpha x^2} \quad ; \quad \tilde{\xi} = 1 - \alpha + \mathcal{O}(\epsilon) \quad ; \quad \alpha^2 = 1 - \frac{\tilde{k}}{2}. \quad (\text{D2})$$



Legendre transforming we find the rate function

$$f(G) = \frac{D(1 - G/\langle G \rangle)^2}{2 \frac{G}{\langle G \rangle}} + \mathcal{O}(1), \quad (\text{D3})$$

where  $\langle G \rangle \simeq 1/4$  in this limit. We are left with determining  $W$  from Eq. (9) or the simpler Eq. (B10) together with Eq. (D2). The final result reads

$$W = 1 + 4r_+ + \mathcal{O}\left[\left(\frac{1}{D}\right)\right]. \quad (\text{D4})$$

### E. Typical dynamics in the weak coupling limit $D \rightarrow 0^+$

Here we explain why at small  $D$ , the typical growth of the total population is dominated by that of patch 1.

At small  $D$  the growth of the population at each patch occurs at a different exponential rate  $\dot{N}_i \simeq (r_i + \eta_i) N_i$  until the population ratio becomes very large  $\mathcal{O}(1/D)$ . At this point the abundance at the faster patch 1 is much larger compared to patch 2 and thus migration to patch 2, relative to population size,  $D(N_2 - N_1)/N_2$  is non-negligible. The migration to patch 1 is negligible because  $N_2$  is small. Indeed, the  $x_-$  distribution at steady state (from Eq. (5) of the main text) is peaked at  $x_- \sim \ln(r_-/D)$ , and the average of migration to patch 1, relative to population size,  $\langle D(N_2 - N_1)/N_1 \rangle$  with respect to this distribution, vanishes to leading order. The same is true for the variance. Thus, the growth of the total population  $N_1 + N_2$  is dominated by that of patch 1 alone with the average growth rate  $r_1$ , which coincides with its zero noise value, and so NIS is negligible here.

### F. Extinction in the weak coupling limit $D \rightarrow 0^+$

Here we present the asymptotic solution of the DV problem (B4) that leads to Eqs. (14)-(15) and to the conditional distributions in Fig. 2(C).

The small  $D$  limit turns out to be a singular perturbation problem with a sharp transition at the critical value of  $k = -2r_-$ . Here the confining potential of the Schrödinger Eq. (B4) becomes very wide with the length scale  $|\ln D|$  and the solution is given by matched asymptotic expansions [57]. The eigenfunction  $\psi$  is characterized by a central non vanishing inner boundary layer, flanked by two outer boundary tails where it decays to zero. The derivation is rather lengthy. We first cite the final results:

The central boundary layer describing the eigenfunction (for  $|x| < |\ln D|$ ) is given by

$$\psi_k^2(x) \simeq \begin{cases} \mathcal{N}_1 e^{-4D \left( \cosh^2 x - \frac{r_- + \frac{k}{2}}{D} x \right)}, & -2r_- < k \leq 0, \quad (\text{F1}) \\ \frac{\mathcal{N}_2}{|\ln D|} e^{-4D \cosh^2 x} \cos^2 \left[ \frac{\pi}{|\ln D|} \left( x + \frac{\psi_{DG}(-\frac{k}{2} - r_-) - \psi_{DG}(-\frac{k}{2} + r_-)}{4} \right) \right], & k \leq -2r_-, \quad (\text{F2}) \end{cases}$$

where  $\psi_{DG}$  is the DiaGamma function,  $\mathcal{N}_{1,2}$  are  $\mathcal{O}(1)$  normalization constants and the first line holds away from a vanishing vicinity of  $-2r_-$ ,  $k + 2r_- = \mathcal{O}(1/\ln D)$ . These expressions are presented in Fig. 2(C) of the main text upon substituting  $k = -W$ , where  $W(r_1, r_2)$  is presented in Eqs.(14)-(15) of the main text.  $W$  can be found using the cumulant generating function (together with (B10)), which is given by

$$\xi(k) \simeq \begin{cases} \frac{k^2}{4} + kr_-, & -2r_- < k \leq 0, \quad (\text{F3}) \\ -r_-^2 + \mathcal{O}\left[\frac{1}{(\ln D)^2}\right], & k \leq -2r_-, \quad (\text{F4}) \end{cases}$$

where the first line holds away from a vanishing vicinity of  $-2r_-$ ,  $k + 2r_- = \mathcal{O}(1/\ln D)$ , and the second line holds except for  $k$  that diverge as  $|k| \sim 1/D$ .

Legendre transforming this expression we have that the rate function  $f(G)$  diverges when  $G$  approaches zero over a vanishing boundary layer  $G \sim \mathcal{O}(1/\ln D)$ , while away from it it is given by the simple parabola

$$f(G) \simeq (G - r_-)^2 \quad ; \quad G > 0. \quad (\text{F5})$$

We now turn to describe the analytical treatment. We solve the eigenvalue problem (B4) separately for  $x \geq 0$  and  $x \leq 0$ , where at each region we invoke matched asymptotics, and then match the solutions. For each region, the relation  $z = 2D \sinh^2 x$  is invertible, and we can substitute

$$\psi(x) = e^{-2D(\cosh^2 x - \frac{r_-}{D}x)} \tilde{\psi}_{\pm}(2D \sinh^2 x), \quad (\text{F6})$$

and arrive at

$$(z^2 + 2Dz) \tilde{\psi}_{\pm}''(z) + (z - 2z^2 + D - 4Dz \pm 2r_- \sqrt{z^2 + 2Dz}) \tilde{\psi}_{\pm}'(z) + kz \tilde{\psi}_{\pm}(z) = \xi \tilde{\psi}_{\pm}(z), \quad (\text{F7})$$

In the following we make expansions in small  $D$  and assume that  $k$  do not scale with  $D$ . Letting  $k$  diverge  $|k| \sim 1/D$  will enable to probe the divergence of  $f$  at the origin.

### 1. Outer solution

Here we assume we have a simple expansion of the solution  $\tilde{\psi}_{\pm}(z) = \tilde{\psi}_0(z) + D\tilde{\psi}_1(z) + \dots$ . Substituting this expansion we have

$$z^2 \tilde{\psi}_{\pm}''(z) + (z - 2z^2 \pm 2r_-) \tilde{\psi}_{\pm}'(z) + kz \tilde{\psi}_{\pm}(z) = \xi \tilde{\psi}_{\pm}(z), \quad (\text{F8})$$

The solution to this equation that does not diverge at infinity, is given by the confluent hypergeometric function  $U$

$$\tilde{\psi}_{\pm}(z) = A z^{\mp r_- + \sqrt{r_-^2 + \xi}} U \left[ \frac{1}{2} \left( 2\sqrt{r_-^2 + \xi} \mp 2r_- - k \right), 1 + 2\sqrt{r_-^2 + \xi}, 2z \right]. \quad (\text{F9})$$

The other independent solution to the ODE (F8) is given by the modified Laguerre function which diverges as  $e^{2z}$  at infinity and is thus invalid. For negative values of  $r_-^2 + \xi < 0$ , the outer solution give way to

$$\tilde{\psi}_{\pm}(z) = A_{\pm} z^{\mp r_- + i\sqrt{-r_-^2 - \xi}} U \left[ \frac{1}{2} \left( 2i\sqrt{-r_-^2 - \xi} \mp 2r_- - k \right), 1 + 2i\sqrt{-r_-^2 - \xi}, 2z \right]. \quad (\text{F10})$$

### 2. Inner region

Now we introduce a boundary layer coordinate  $\tilde{z} = Dz$ , and expanding in the near region

$$\tilde{\psi}_{\pm}(z) = v(\tilde{z}) + Dv_1(\tilde{z}) + \dots \quad (\text{F11})$$

Plugging it into (F7) we arrive at

$$(\tilde{z}^2 + 2\tilde{z}) v_{\pm}''(\tilde{z}) + (\tilde{z} + 1 \pm 2r_- \sqrt{\tilde{z}^2 + 2\tilde{z}}) v_{\pm}'(\tilde{z}) = \xi v_{\pm}(\tilde{z}). \quad (\text{F12})$$

There are two independent solutions to this equation

$$v_{\pm}(\tilde{z}) = \frac{B_{\pm} \left( \sqrt{\frac{\tilde{z}}{2}} + \sqrt{1 + \frac{\tilde{z}}{2}} \right)^{2\sqrt{r_-^2 + \xi}} + C_{\pm} \left( \sqrt{\frac{\tilde{z}}{2}} + \sqrt{1 + \frac{\tilde{z}}{2}} \right)^{-2\sqrt{r_-^2 + \xi}}}{\left[ 1 + \tilde{z} + \sqrt{\tilde{z}(2 + \tilde{z})} \right]^{\pm r_-}} \quad (\text{F13})$$

For negative values of  $r_-^2 + \xi < 0$ , the inner solution give way to

$$v_{\pm}(\tilde{z}) = \frac{D_{\pm} \cos \left[ 2\sqrt{-r_-^2 - \xi} \operatorname{arcsinh} \left( \sqrt{\frac{\tilde{z}}{2}} \right) + \varphi_{\pm} \right]}{\left[ 1 + \tilde{z} + \sqrt{\tilde{z}(2 + \tilde{z})} \right]^{\pm r_-}}. \quad (\text{F14})$$

The  $\pm$  solutions for  $v_{\pm}$  must be matched at  $x = 0$ . As the denominator gives in the original variables

$$\left[ 1 + \tilde{z} + \sqrt{\tilde{z}(2 + \tilde{z})} \right]^{\pm r_-} = e^{2r_- x}, \quad (\text{F15})$$

we must have that

$$B_+ = C_- \quad ; \quad B_- = C_+ \quad ; \quad D_+ = D_- \quad ; \quad \varphi_+ = -\varphi_- \quad (\text{F16})$$

We are left with matching the outer solutions  $\tilde{\psi}_{\pm}$  with the inner ones  $v_{\pm}$  by employing a matching condition.

### 3. Matching the inner and outer solutions

There are two different regimes here:

$$4. \quad -r_-^2 < \xi \leq 0$$

In this case we find that the outer solution diverges at the origin. the first two terms are given by:

$$\begin{aligned} \tilde{\psi}_\pm(z \rightarrow 0) \simeq A_\pm z^{\mp r_-} \frac{\Gamma(-2\sqrt{r_-^2 + \xi})}{\Gamma\left[-\frac{1}{2}\left(2\sqrt{r_-^2 + \xi/\sigma^2} + k \pm 2r_-\right)\right]} \times \\ \left[ z^{\sqrt{r_-^2 + \xi/\sigma^2}} + z^{-\sqrt{r_-^2 + \xi/}} \frac{2^{-2\sqrt{r_-^2 + \xi}} \Gamma(2\sqrt{r_-^2 + \xi})}{\Gamma\left[\frac{1}{2}\left(2\sqrt{r_-^2 + \xi} - k \mp 2r_-\right)\right]} \frac{\Gamma\left[-\frac{1}{2}\left(2\sqrt{r_-^2 + \xi} + k \pm 2r_-\right)\right]}{\Gamma(-2\sqrt{r_-^2 + \xi})} \right], \end{aligned} \quad (\text{F17})$$

where  $\Gamma$  is the gamma function. Expanding the inner solution at infinity we find two matching terms:

$$v_\pm(\tilde{z} \rightarrow \infty) \simeq z^{\mp r_-} (2D)^{\mp r_- + \sqrt{r_-^2 + \xi}} \left[ B_\pm z^{\sqrt{r_-^2 + \xi}} + \frac{D^{2\sqrt{r_-^2 + \xi}}}{2^{2\sqrt{r_-^2 + \xi}}} C_\pm z^{-\sqrt{r_-^2 + \xi}} \right]. \quad (\text{F18})$$

Then the matching condition reads:

$$\frac{\Gamma(2\sqrt{r_-^2 + \xi})}{\Gamma(-2\sqrt{r_-^2 + \xi})} \frac{\Gamma\left[-\frac{1}{2}\left(2\sqrt{r_-^2 + \xi} + k \pm 2r_-\right)\right]}{\Gamma\left[\frac{1}{2}\left(2\sqrt{r_-^2 + \xi} - k \mp 2r_-\right)\right]} = D^{2\sqrt{r_-^2 + \xi}} \frac{C_\pm}{B_\pm} \quad (\text{F19})$$

Employing the relation (F16) we arrive at

$$\left[ \frac{\Gamma(2\sqrt{r_-^2 + \xi})}{\Gamma(-2\sqrt{r_-^2 + \xi})} \right]^2 \frac{\Gamma\left[-\frac{1}{2}\left(2\sqrt{r_-^2 + \xi} + k - 2r_-\right)\right]}{\Gamma\left[\frac{1}{2}\left(2\sqrt{r_-^2 + \xi} - k + 2r_-\right)\right]} \frac{\Gamma\left[-\frac{1}{2}\left(2\sqrt{r_-^2 + \xi} + k + 2r_-\right)\right]}{\Gamma\left[\frac{1}{2}\left(2\sqrt{r_-^2 + \xi} - k - 2r_-\right)\right]} = D^{4\sqrt{r_-^2 + \xi}} \quad (\text{F20})$$

Except for vanishing  $r_-^2 + \xi = \mathcal{O}(1/\ln D)$ , the leading order in  $D$  is achieved when the left hand side vanishes. That is either  $2\sqrt{r_-^2 + \xi} - k - 2r_- = 0$  or  $2\sqrt{r_-^2 + \xi} - k + 2r_- = 0$ . As  $k \leq 0$ , only the first option can hold and we finally have that for  $-2r_- < k \leq 0$

$$\xi \simeq \frac{k^2}{4} + kr_-, \quad (\text{F21})$$

which holds accept for  $k$  in small vicinity of  $-2r_-$ ,  $k + 2r_- = \mathcal{O}(1/\ln D)$ .

In addition, we have the following matching for the coefficients

$$A_+ = B_+ \left(\frac{2}{D}\right)^{-r_- + \sqrt{r_-^2 + \xi}} \frac{\Gamma\left[-\frac{1}{2}\left(2\sqrt{r_-^2 + \xi} + k + 2r_-\right)\right]}{\Gamma(-2\sqrt{r_-^2 + \xi})} \quad (\text{F22})$$

which in light of the relation (F21) is reduced to

$$A_+ = B_+ \left(\frac{2}{D}\right)^{\frac{k}{2}}. \quad (\text{F23})$$

We also deduce that

$$C_+ = B_+ D^{k+2r_-} \frac{\Gamma(-k-2r_-) \Gamma(2r_-)}{\Gamma(k+2r_-) \Gamma(-k)} \quad (\text{F24})$$

and from the matching of the  $-$  parts we also find

$$A_- = B_- \left( \frac{2}{D} \right)^{2r_- + \frac{k}{2}} \frac{\Gamma(-k)}{\Gamma(-k - 2r_-)} = B_+ 2^{2r_-} (2D)^{\frac{k}{2}} \frac{\Gamma(2r_-)}{\Gamma(k + 2r_-)} = A_+ 2^{2r_-} D^k \frac{\Gamma(2r_-)}{\Gamma(k + 2r_-)}. \quad (\text{F25})$$

Importantly, as  $C_+$  is negligible compared to  $B_+$ , we have that the inner region is approximated by

$$\psi^2(x) \simeq \mathcal{N} e^{-4D \left( \cosh^2 x - \frac{r_- + \frac{k}{2}}{D} x \right)}, \quad (\text{F26})$$

This approximation breaks down when  $k$  approaches  $-2r_-$  as  $C_+$  is no longer negligible.

### 5. $\xi \leq -r_-^2$

In this case we find that the square root  $\sqrt{\xi + r_-^2}$  becomes imaginary and the outer solution is expended at the origin by:

$$\begin{aligned} \tilde{\psi}_\pm(z \rightarrow 0) &\simeq \frac{A_\pm z^{\mp r_-}}{2^{i\sqrt{-\xi - r_-^2}}} \left[ (2z)^{i\sqrt{-r_-^2 - \xi}} \alpha_\pm^* + (2z)^{-i\sqrt{-r_-^2 - \xi}} \alpha_\pm \right] + \dots \\ &= \frac{A_\pm z^{\mp r_-}}{2^{i\sqrt{-\xi - r_-^2}}} |\alpha_\pm| \cos \left[ \sqrt{-r_-^2 - \xi} \ln(2z) - \arg \alpha_\pm + \dots \right] \end{aligned} \quad (\text{F27})$$

where

$$\alpha_\pm = \frac{\Gamma\left(2i\sqrt{-\xi - r_-^2}\right)}{\Gamma\left[\frac{1}{2}\left(2i\sqrt{-\xi - r_-^2} - k \mp 2r_-\right)\right]}. \quad (\text{F28})$$

For the inner solution we find

$$v_\pm(\tilde{z} \rightarrow \infty) \simeq D_\pm \left( \frac{D}{2} \right)^{\pm r_-} z^{\mp r_-} \cos \left[ \sqrt{-r_-^2 - \xi} \ln \left( \frac{2z}{D} \right) + \varphi_\pm + \dots \right] \quad (\text{F29})$$

The matching condition than reads

$$\begin{aligned} \arg \alpha_+ + \arg \alpha_- = \\ \arg \left[ \frac{\Gamma\left(2i\sqrt{-\xi - r_-^2}\right)}{\Gamma\left[\frac{1}{2}\left(2i\sqrt{-\xi - r_-^2} - k - 2r_-\right)\right]} \right] + \arg \left[ \frac{\Gamma\left(2i\sqrt{-\xi - r_-^2}\right)}{\Gamma\left[\frac{1}{2}\left(2i\sqrt{-\xi - r_-^2} - k + 2r_-\right)\right]} \right] = 2\sqrt{-r_-^2 - \xi} \ln D \end{aligned} \quad (\text{F30})$$

and the phases are given by

$$\varphi_+ = -\varphi_- = \frac{\arg \alpha_- - \arg \alpha_+}{2}. \quad (\text{F31})$$

Notice, that from the matching condition (F30) we have the scaling

$$\sqrt{-r_-^2 - \xi/\sigma^2} \sim \frac{1}{\ln D}. \quad (\text{F32})$$

Using the above scaling, we can expand the Gamma functions in the left hand side of (F30). Carefully collecting terms for the real and imaginary parts, we have the approximate matching condition

$$\arg \left[ -\psi_{DG} \left( -\frac{k}{2} - r_- \right) - 2\gamma - \frac{i}{\sqrt{-r_-^2 - \xi}} \right] + \arg \left[ -\psi_{DG} \left( -\frac{k}{2} + r_- \right) - 2\gamma - \frac{i}{\sqrt{-r_-^2 - \xi}} \right] = 2\sqrt{-r_-^2 - \xi} \ln D \quad (\text{F33})$$

where  $\gamma$  is the Euler–Mascheroni constant, and  $\psi_{DG}$  is the DiaGamma function. Let us substitute than  $\xi = -r_-^2 - \frac{\tilde{\xi}}{(\ln D)^2}$

$$\arg \left[ -\psi_{DG} \left( -\frac{k}{2} - r_- \right) - 2\gamma + i \frac{\ln D}{\sqrt{\tilde{\xi}}} \right] + \arg \left[ -\psi_{DG} \left( -\frac{k}{2} + r_- \right) - 2\gamma + i \frac{\ln D}{\sqrt{\tilde{\xi}}} \right] = -2\sqrt{\tilde{\xi}}. \quad (\text{F34})$$

To find  $\varphi_+$  (F31) we must solve for  $\alpha_{+,-}$ . To leading order at small  $D$  we have that, apart for  $k$  close to  $-2r_-$ , the arguments of  $\alpha_{+,-}$  both approach  $-\pi/2$  and so  $\varphi_+$  vanishes for  $k$  away from a narrow boundary layer around  $-2r_-$ . Beyond that boundary layer, the next order expansion reads  $2\varphi_+ |\ln D| = \frac{\pi}{4} [\psi_{DG}(-\frac{k}{2} - r_-) - \psi_{DG}(-\frac{k}{2} + r_-)] + \mathcal{O}[\frac{1}{\ln D}]$ . All and all, we can conclude that to leading order the central part is given by

$$\psi^2 \simeq \frac{\mathcal{N}}{|\ln D|} e^{-4D \cosh^2 x} \cos^2 \left[ \frac{\pi}{|\ln D|} \left( x + \frac{\psi_{DG}(-\frac{k}{2} - r_-) - \psi_{DG}(-\frac{k}{2} + r_-)}{4} \right) \right], \quad (\text{F35})$$

where  $\mathcal{N}$  is an  $\mathcal{O}(1)$  normalization constant.

### G. Conditioned dynamics in the weak coupling limit $D \rightarrow 0^+$

Here we derive Eqs. (12) and (13).

In the extinction sink regime  $r_2 \leq -r_1$ , we have that the optimal value of  $G$  (from Eq. (9) of the main text) is given by  $G = -r_+$  which corresponds to  $k = -2r_1 > -2r_-$ . Thus, the corresponding eigenfunction is given by expression (F26).

Plugging these results in Eq. (10) and (11) of the main text we find

$$\dot{x}_-^c = -r_+ - D \sinh 2x_- + \frac{1}{\sqrt{2}} \eta_-, \quad (\text{G1})$$

and

$$\dot{x}_+^c = 2D \sinh^2 x_- (t) + r_+ - \frac{x_+}{T-t} + \frac{1}{\sqrt{2}} \eta_+, \quad (\text{G2})$$

from which we obtain

$$\dot{x}_1^c = -\frac{x_1^c + x_2^c}{2(T-t)} + D \left( e^{x_2^c - x_1^c} - 1 \right) + \eta_1, \quad (\text{G3})$$

$$\dot{x}_2^c = -\frac{x_1^c + x_2^c}{2(T-t)} + (r_1 + r_2) + D \left( e^{x_1^c - x_2^c} - 1 \right) + \eta_2. \quad (\text{G4})$$

Just as for the typical growth, during extinction the abundance in patch 2 is much smaller than in patch 1, and the migration to patch 1 can be neglected. This means we can set the second term in the right hand side of Eq. (G3) to zero. Indeed, the  $x_-^c$  distribution obtained from Eq. (G1) is localized around  $x_-^c \sim \ln(-r_+/D) \gg 1$ , and the average, and variance of this term vanishes to leading order. Now we also rewrite the Eq. (G3) as:

$$\dot{x}_1^c = -\frac{x_1^c}{(T-t)} + r_1 \frac{x_-^c}{\ln K (1 - r_1 t / \ln K)} + \eta_1, \quad (\text{G5})$$

where we also substituted the decline rate  $r_d = r_1$ . As  $x_-^c = \mathcal{O}(1)$  (do not scale with  $\ln K$ ), than apart from narrow Boundary layer in time of width  $r_1^{-1} \ll T$  around  $t = T$ , the  $x_-^c$  term can be neglected, and we arrive at the Eq. (12) of the main text.

In the same way, we replace the first term on the right-hand side of Eq. (G4) by  $-x_1^c / (T-t)$ , which can be further approximated by its average  $-r_1$ . To prove the previous statement we make use of the exact solution for the  $x_1^c$  distribution which follows from Eq. (12) of the main text

$$P(x_1^c, t) = \frac{1}{\sqrt{2\pi t(1-t/T)}} e^{-\frac{[x_1^c - r_1(T-t)]^2}{2t(1-t/T)}}, \quad (\text{G6})$$

and so we have that the distribution of  $-x_1^c/(T-t)$  is given by

$$P[x_1^c/(T-t) = \tilde{r}, t] = \frac{1}{\sqrt{2\pi\tilde{\sigma}^2(t)}} e^{-\frac{(\tilde{r}-r_1)^2}{2\tilde{\sigma}^2(t)}}, \quad (\text{G7})$$

where

$$\tilde{\sigma}^2(t) = \frac{1}{T} \frac{t/T}{1-t/T} = \frac{r_1}{\ln K} \frac{t/T}{1-t/T}. \quad (\text{G8})$$

Thus, apart from a narrow boundary layer in time around  $t = T$  of width  $r_1^{-1} \ll T$ , the variance scales as  $1/\ln K$  and is vanishingly small. Approximating  $-\frac{x_1^c + x_2^c}{2(T-t)} \simeq -r_1$  in the Eq. (G4) we arrive at Eq. (13) of the main text.

## H. Non constant potential $U'(x_+)$ in Eq. (16)

Here we look at rare events for the dynamics

$$\begin{aligned} \dot{x}_+ &= -U'(x_+) + g(x_-) + \sigma_+ \eta_+, \\ \dot{x}_- &= -V'(x_-) + \sigma_- \eta_-, \end{aligned} \quad (\text{H1})$$

with non constant  $U'$ . We look at rare events of (H1) in which the reaction coordinate  $x_+$  reaches a large potential difference  $\Delta U/\sigma_+^2 \gg 1$ . For a *given*  $x_-(t)$  trajectory, the probability cost of the  $x_+$  histories in this case are given within the IM formalism where one minimizes the *conditional* action of the  $x_+$  path probability measure  $S_+[x_+(t)|g(t)] = \int dt [x_+ + U'(x_+) - g(x_-)]^2/2\sigma_+^2$ . However, the accompanying  $x_-$  trajectories are not dominated by a single path and IM is inapplicable.

Instead, if the rare  $x_+$  history varies over a time scale  $\mathcal{T}$  which is much larger compared to the fast relaxation time  $\tau$  of  $x_-$  inside the potential  $V_-$ , then the accompanying  $x_-$  histories can be found within the DV formalism. Denote the time average  $G(t) = \int_{t-T/2}^{t+T/2} g[x_-(t')] dt'/T$ , over an intermediate time scale  $\tau \ll T \ll \mathcal{T}$ . Then the probability of observing any fluctuations in  $G$  decays exponentially with  $T - \ln P \simeq Tf(G)$ , where the rate function  $f$  is given within the DV large deviation formalism. Correspondingly, for any given protocol  $G(t)$ , which varies over the slow time scale  $\mathcal{T}$ , its probability is evaluated by the time integral  $-\ln P \simeq S_{\text{DV}} = \int dt f[G(t)]$

Next, as the  $x_+$  dynamics is characterized by the same slow time scale, we can safely replace  $g(x_-)$  in the conditional path probability measure by the segmented time average given by  $G(t)$ . Putting everything together, we find that the unconditional probability of observing the large deviation of interest is given by the hybrid minimization problem for the sum of the IM action and DV large deviation function  $-\ln P \simeq \min_{x_+(t), G(t)} \{S_+[x_+|G] + S_{\text{DV}}(G)\}$ . We see that the usual IM action for the  $x_-$  paths is replaced here by the DV large deviation function. Most importantly, the DV theory gives access to the histories of the system conditioned on the large deviation of interest.

## I. Specialized forms with simplifying features

For linear  $V$ ,  $x_-$  is an Ornstein–Uhlenbeck process. If, in addition,  $g$  is also linear then one can show that the time average  $G = \int_0^T dt g(t)/T$ , over a long times  $T$ , is a Gaussian variable. As such, it displays the usual IM small noise scaling. As a result, the IM happens to correctly reproduce the large deviation for rare events, however without an account of the fluctuating dynamics conditioned on the rare event. This simpler case appeared in several previous works such as [36, 38].

Yet even when  $x_-$  is an Ornstein–Uhlenbeck process, once  $g$  is nonlinear then the IM is in general inapplicable. However, for the special case where it is quadratic  $g \propto x^2$  then the biased path integral that corresponds to conditioning the process (H1) on a given time average of  $g$  is a Gaussian path integral which can be evaluated exactly. This simplification was used in [48], however, without addressing the dynamics.

For general non-Gaussian noise (non-linear  $V(x), g(x)$ ), and for addressing the dynamics, one must resort to the hybrid DV and IM formalism.